Rheological Properties of Progesterone Microemulsions: Influence of Xanthan and Chitosan Biopolymer Concentration

F. Corrias,[1] M. Dolz,[2] M. Herraez,[1] O. Diez-Sales[1]

[1]*Department of Pharmacy and Pharmaceutical Technology, Faculty of Pharmacy, University of Valencia, Vicente Andrés Estellés s/n, 46100-Burjassot (Valencia), Spain*
[2]*Department of Earth Physics and Thermodynamics, Faculty of Physics, University of Valencia, Vicente Andrés Estellés s/n, 46100-Burjassot (Valencia), Spain*

Received 2 October 2007; accepted 24 April 2008
DOI 10.1002/app.28657
Published online 11 July 2008 in Wiley InterScience (www.interscience.wiley.com).

ABSTRACT: In this preformulations study, rheological properties of microemulsions with progesterone (1%) were studied to analyze the effect of xanthan and chitosan at different concentrations (0.5–3%). Steady shear and oscillatory rheological properties were analyzed using a controlled stress rheometer. Steady shear data were satisfactorily adjusted to the Carreau model. For all preparations, shear-thinning behavior was observed. Zero shear viscosity (η_0) increased with the biopolymer concentration. The results from dynamic experiments showed the behavior of all preparations with xanthan gum and those of chitosan to be characteristic of weak gels and liquid-like solutions, respectively. The correlation between dynamic and steady-shear properties (extended Cox-Merz rule) was satisfactory for the two polymers. The recovery analysis of microemulsions with xanthan showed a total recovery percentage of 90% for the highest concentrations of this polymer. However, microemulsions with chitosan showed practically no recovery. Progesterone release was greater for the microemulsions with chitosan. © 2008 Wiley Periodicals, Inc. J Appl Polym Sci 110: 1225–1235, 2008

Key words: microemulsions; biopolymers; viscoelasticity; flow curves; drug delivery systems

INTRODUCTION

The topical application of sex hormones to selected skin sites might be an alternative for hormone replacement in postmenopausal skin, thereby slowing the ageing process that rapidly progresses with the onset of menopause. The steroid structure of the sex hormones and their high lipid solubility makes them suitable for a percutaneous route of administration. It is already known that estrogen and its derivates increase collagen production and epidermal hydration in the skin, and reduce the typical signs of ageing such as wrinkling and elastosis.[1–3] Recently, the effect of progesterone cream (O/W and W/O) on the skin of peri- and postmenopausal women has been studied.[4] The results of this study demonstrate that the topical application of progesterone cream primarily acts by increasing skin elasticity and firmness in peri- and postmenopausal women.

On the other hand, in attempt to increase cutaneous drug delivery, microemulsions formulations have been shown to be superior for both transdermal and dermal delivery of particular lipophilic compounds, but also hydrophilic compounds appear to benefit from applications in microemulsions compared with conventional vehicles, such as hydrogels, liposomes, and emulsions.[5,6] Therefore, microemulsions represent an interesting prospect for the development of formulations for use as vehicles to deliver drugs to the human body.[7,8]

In addition numerous studies have been conducted using various lecithin-based microemulsions as topical formulations enhancing the penetration of different drugs: methotrexate,[9] diclofenac,[10] indomethacin,[11] etc. Absorption of phospholipids on skin can increase tissue hydration, consequently increasing drug permeation. When phospholipids are applied to skin as vehicles due to their physicochemical properties and structures they can fuse with the stratum corneum lipids, perturb its structure, and facilitate drug delivery.[12] Another advantage of these surfactants is the possibility of forming microemulsions without cosurfactants. In this context, lesser surfactants are associated with lesser irritation. Beyond it, most microemulsions are of a very low viscosity therefore their use may be restricted.

On the other hand, it is well known that biopolymers can act to increase the consistence and the

Correspondence to: O. Diez-Sales (octavio.diez@uv.es).

stability of emulsions. For this purpose chitosan and xanthan were chosen. Chitosan is known to be biocompatible and biodegradable[13] and at physiological pH is also bioadhesive, which increases its retention at the site of application.[14] Chitosan also promotes wound healing[15] and possesses bacteriostatic effects.[16] Both polysaccharides can be used to stabilize pharmaceutical emulsions[17] and for controlled-release drug delivery.[18,19]

The aim of this article, based on a progesterone microemulsion without cosurfactants, is to investigate the influence of different concentrations of xanthan and chitosan upon the rheological properties of these formulations and the release rate of progesterone—a lipophilic model compound—through an artificial membrane.

EXPERIMENTAL

Materials

Sesame oil (lot 944790003), soybean lecithin grain (lot 9386900016), glycerin (lot 914290001), methylparaben (lot 9243600018), and progesterone (lot 9368500020) were purchased from Guinama (Valencia, Spain). Xanthan gum (lot 035k0199) with a molecular weight ($\sim 3 \times 10^5$ g/mol) and chitosan with average molecular weight of 7.5×10^5 g/mol (75–85% deacetylated) (lot 01518AD) were purchased from Sigma Chemical (Madrid, Spain). Water purified by reverse osmosis (MilliQ® Millipore, Spain) and with a resistivity above 18.2 MΩ cm was used. All other chemicals were of high-performance liquid chromatography (HPLC) analytical grade.

Formulations

Microemulsions of progesterone (1%, w/w) were prepared. The manufacturing method comprised of two stages: the first dealt with microemulsion formation and the second the addition of different concentrations of xanthan or chitosan (from 0.5 to 3%, w/w) in the microemulsion.

In the first stage, the oil phase (O) with soybean lecithin (1%, w/w), sesame oil (10%, w/w), and progesterone (1%, w/w) was prepared. The oil phase was homogenized with an ultrasonic bath (Ultrasonic cleaned-Fungilab, for 30 min at 45°C). The aqueous phase (W) was also prepared in two different containers: glycerin (2.5%) was mixed in purified water (42.7%) with methylparaben (0.1%) (W_1). In turn, W_1 was added to O, and emulsification was carried out using a rotor-stator Ultraturrax (DI25-basic, IKA-Germany), with a homogenization speed of 5000 rpm during 5 min. Then, the emulsion (O/W) was treated (3 cycles of 10 min) with an Ultrasonic generator Soniprep 150 (23 kHz) equipped with a Titanium Probe (end diameter 9.5 mm) and a Process Timer Unit, allowing us to program the experiments in terms of the total duration of treatment and the preselected cycling of alternate bursts of sonication/cooling, also equipped with a continuous Flow Vessel 48533-1016. This vessel is surrounded by a cooling jacket with a suitable cooling liquid.

In the second stage, in another container, the proper amount of xanthan or chitosan was mixed in water purified up to 100 g of preparation (W_2). Finally, W_2 was mixed with the microemulsion under agitation and maintained during 7 days at 25°C, until measurement.

This method allows the preparation of a stable microemulsion with different consistencies according to the concentration of xanthan and chitosan used.

Drop size distribution and zeta potential

The drop size distribution of progesterone microemulsions was determined by the laser light scattering technique (Zetasizer Nano Series, Malvern Instruments, United Kingdom), which is able to determine the Zeta potential and discriminate drop sizes in the interval 0.6 nm to 6 μm, using distilled water (1:10) as dispersant medium. The average diameter used to describe the results of the drop size distribution is the Sauter diameter D (3,2) defined as[20]:

$$D(3,2) = \frac{\sum d^3}{\sum d^2} \quad (1)$$

Rheological characterization

A Haake Rheostress 1 rheometer (Thermo Haake, Germany) with data acquisition software (RheoWin 2.94) and a circulator for sample temperature control was used. Samples were allowed to rest for at least 300 s prior to analysis. In all cases, the exposed edges of the sample were covered with silicone oil (Dimethicone RFE/Ph. Eur.) to prevent evaporation of water during measurement. All measurements were made in triplicate at 25°C.

Flow curves

The rheological measurements were carried out using a cone-plate (2°, 35 mm diameter) for microemulsions with xanthan or chitosan concentrations from 0.5% to 3%, while for the rest of microemulsions serrated plates (35 mm diameter and 1 mm gap) were used to avoid slippage. Steady-state flow curves were obtained working in controlled stress mode. Different ranges of shear stresses, in logarithmic distribution, were used to obtain shear rates between 0.0001 and 1000 s^{-1}, approximately. This

variation in viscosity with shear rate was fitted with the simplified Carreau model.[21]

$$\eta = \frac{\eta_0}{\left[1 + \left(\frac{\dot{\gamma}}{\gamma_c}\right)^2\right]^c} \quad (2)$$

where η_0 is the zero-shear viscosity (Pa s), the constant viscosity in the lower Newtonian plateau; γ_c is the critical shear rate corresponding to the transition from Newtonian to shear-thinning behavior (s^{-1}); c is equal to $(1 - n)/2$ and n is a dimensionless constant that corresponds to the power law index or flow index.

Oscillatory test

In all cases, the rheological measurements were carried out using a cone-plate (2°, 35 mm diameter). To determine the linear viscoelastic range, stress sweeps at 25°C and at a frequency of 1 Hz were performed for all systems studied. Frequency sweep tests were performed from 0.01 Hz (0.0693 rad/s) to 10 Hz (69.3 rad/s), and in a range from 0.3 to 1 Pa. The oscillatory parameters used to compare the viscoelastic properties for all the systems were the storage modulus (G'), the loss modulus (G''), the loss tangent ($\tan \delta = G''/G'$) and complex viscosity (η^*).

Creep and recovery

Creep and recovery analyses for the microemulsions were also carried out under the same experimental conditions mentioned above. A constant stress in the linear region was applied instantly and maintained for a period of 300 s (creep), and compliance was measured. After removing the stress, compliance values were also measured during 300 s (recovery).

For microemulsions with xanthan gum, the creep data were analyzed according to the Burger model [eq. (3)], consisting of one Maxwell unit and one Kelvin-Voigt unit in series.[22]

$$J(t) = \frac{1}{G_o} + \frac{1}{G_1}\left[1 - \exp\left(\frac{-t \cdot G_1}{\eta_1}\right)\right] + \frac{t}{\eta_o} \quad (3)$$

$J(t)$ represents the overall compliance at any time t, G_0 is the instantaneous elastic modulus of the Maxwell unit, and G_1 is the elastic modulus of the Kelvin-Voigt unit. The latter represents the contributions of the retarded elastic region to the total compliance. The dashpot of the Maxwell element represents the residual viscosity, η_0, and the dashpot associated with Kelvin-Voigt is called the internal viscosity, η_1.

In the case of microemulsions with chitosan, the creep data were analyzed according to the Maxwell model [eq. (4)].

$$J(t) = \frac{1}{G_o} + \frac{t}{\eta_o} \quad (4)$$

The experimental values of compliance J (Pa^{-1}) in the recovery process for microemulsions with xanthan were fitted with the following empirical equation[23]:

$$J(t) = J_\infty + J_{KV} \exp\left(-Bt^C\right) \quad (5)$$

where B and C are parameters which define the recovery rate of the system, J_∞ is the residual compliance, J_{KV} is the maximum compliance of the Kelvin-Voigt element, and t is time.

Additionally, Maxwell's spring deformation, or initial shear compliance J_0, was obtained by using eq. (6), where J_{MAX} is the maximum deformation corresponding to the experimental compliance value for the longest time (300 s) in the creep transient analysis.

$$J_O = J_{MAX} - (J_\infty + J_{KV}) \quad (6)$$

On the other hand, the experimental values of compliance J (Pa^{-1}) in the recovery process for microemulsions with chitosan were not fitted, because there was practically no recovery.

The fitting procedure was carried out by means of KaleidaGraph nonlinear regression (Synergy Software© KaleidaGraph, version 3.51).

In vitro drug release

Drug delivery investigations with topical microemulsions have been done *in vitro*, using the classical Franz-type diffusion cells.[8] Progesterone release rates from the microemulsions with xanthan gum or chitosan (containing 1 and 2%, w/w) were determined through 0.45 mm cellulose-acetate membrane filters (Teknocroma, Barcelona, Spain), using Franz type cells[8] with an available diffusion area of 0.78 cm^2 and 6 mL of receptor cell volume, placed in heating/stirring mode.[24] Because of the slight solubility of progesterone in aqueous solution, the receptor compartments were filled with distilled water in ethanol (50 : 50), and the receptor phase was stirred with small magnetic bars. To attain 32°C at the membrane surface, the receptor phase was maintained at (37 ± 0.5)°C. Subsequently, the microemulsion (500 mg) was placed on the artificial membrane and covered with parafilm to prevent evaporation. At predetermined time intervals, 100 μL samples

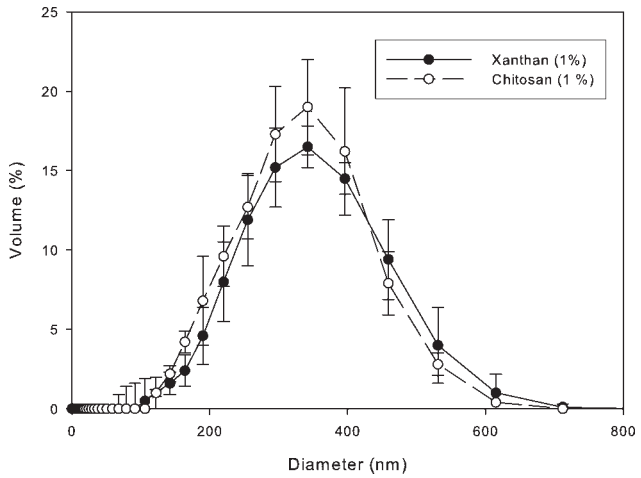

Figure 1 Particle size distribution for the microemulsion with 1% of xanthan gum and a microemulsion with chitosan (1%) ($n = 5$).

were taken from the receptor and replaced by the same volume of fresh liquid to maintain constant volume.

The mean release profiles were fitting according to the power law equation to describe the drug release mechanism from the microemulsions examined[25]:

$$\frac{M_t}{M_\infty} = K \cdot t^n \tag{7}$$

where M_t and M_∞ are the absolute amount of drug released at t and infinite time, respectively; K is a constant reflecting structural and geometric characteristic of the device, and n is the release exponent characterizing the diffusional mechanism. When $n = 0.5$, the fraction of the drug released is proportional to the square root time (Higuchi equation), and drug release is pure diffusion controlled; when $n = 1$, drug release exhibits zero order kinetics or case-II transport. Values of n between 0.5 and 1 indicate anomalous transport and the superposition of both phenomena.[25]

Determination of progesterone

The method used for progesterone determination is based on the procedure proposed by Lindholm et al.[26] The samples were analyzed by HPLC (Hewlett–Packard 1100) with ultraviolet detection ($\lambda = 245$ nm). The column used was a reversed-phase Kromasil C-18 5 μm 150 × 4.6 mm (Ref: L1415, Analisis Vinicos S.L., Tomelloso, Spain). The mobile phase consisted of acetonitrile/water (80 : 20), and the flow rate was 1.0 mL/min.

Statistical analysis

Homogeneity was confirmed by the Barlett test. One-way ANOVA, followed by the Tukey multiple comparison test was performed with the representative values of particle size, progesterone release and rheological parameters, to establish differences between the calculated means (SPSS 12.0 statistical package).

RESULTS AND DISCUSSION

Drop size distribution

As an example of particle size distribution, the results obtained for microemulsions with xanthan (1%) and chitosan (1%) are shown in Figure 1. In turn, Table I summarizes the mean drop size values and standard deviations obtained for the different microemulsions. The result for microemulsion without polymer was 306 ± 15 nm, and there were no significant differences ($P > 0.05$) with the different microemulsions. The Zeta potential values for these concentrations of these biopolymers have also been summarized in Table I. Obviously, in accordance with the nature of these polymers, the values are negative for microemulsions with xanthan and positive for microemulsions with chitosan.

Flow curves

Typical flow curves at 25°C for the preparations, at different concentrations of xanthan and chitosan, are

TABLE I
Drop Size and Zeta Potential for the Microemulsions with Xanthan and Chitosan

Conc. (%, w/w)	Xanthan		Chitosan	
	Size (nm)	Z. Potential (mV)	Size (nm)	Z. Potential (mV)
0.5	303 ± 18	−36.8 ± 1.6	317 ± 15	+42.4 ± 2.1
1.0	323 ± 17	−32.6 ±0.9	305 ± 21	+40.1 ± 2.3
1.5	314 ± 16	−19.1 ± 1.4	310 ± 17	+36.7 ± 1.4
2.0	301 ± 12	−11.4 ±0.5	299 ± 15	+33.8 ± 3.1
2.5	311 ± 14	−17.1 ± 0.8	318 ± 16	+34.1 ± 1.9
3.0	305 ± 22	−19.6 ± 1.2	312± 25	+34.7 ± 1.5

Results are the mean ± standard deviations ($n = 5$).

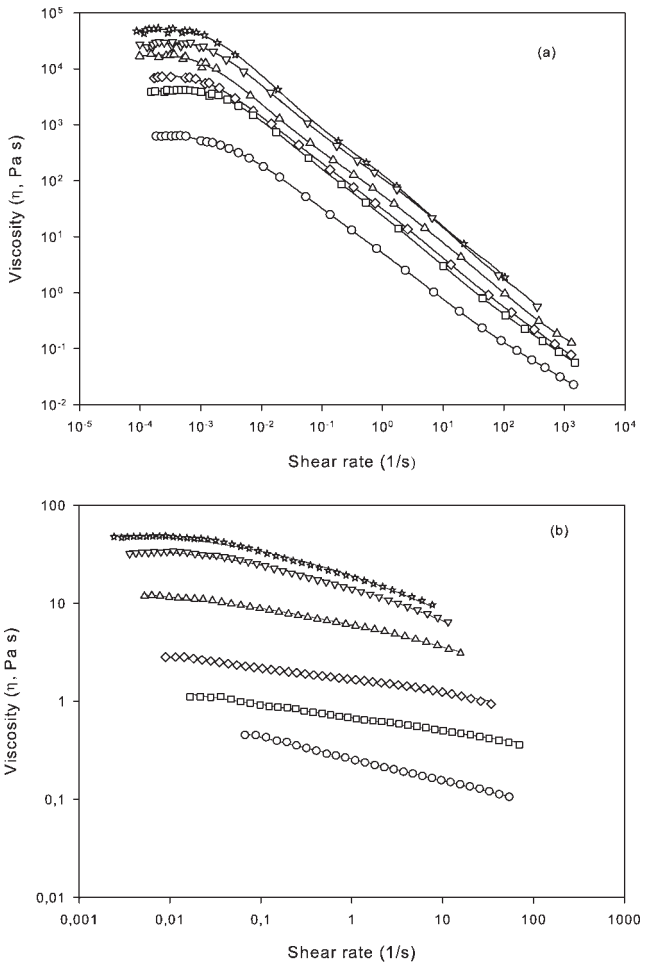

Figure 2 Flow curves at different concentrations of xanthan (a) and chitosan (b) for the microemulsions: 0.5% (-o-), 1% (-□-), 1.5% (-◇-), 2% (-Δ-), 2.5% (-▽-) and 3% (-☆-).

shown in Figure 2. In this figure, the continuous lines are the fits to the simplified Carreau's model [eq. (2)]. Agreement with the experimental data is quite satisfactory, as can be seen in the figure. In all cases, the regression coefficient, r, was $\geq$0.996. The values obtained for zero-shear viscosity (η_0, Pa s), $\dot{\gamma}_c$ (s^{-1}) and c are shown in Table II. As can be observed the η_0 values of the microemulsiones with xanthan are higher than the η_0 values of the microemulsions with chitosan (Table II), although the chitosan has an average molecular weight twice superior to the xanthan. These differences could be explained taking in consideration that local conformational ordering and lateral association of ordered chain sequences could give place to a weak gel-like network.[27]

In all cases, the behavior was shear-thinning with a Newtonian region in the low shear rate range. The shear-thinning behavior may be regarded as arising from modifications in macromolecular organization in the microemulsions as the shear rate changes. At low shear rates, the disruption of entanglements by the imposed shear is balanced by the formation of new ones, so that no net change in entanglements occurs; it is in the Newtonian plateau region where the viscosity has a constant value (η_0). The values calculated for η_0 increase as the concentration of biopolymer increases, the highest viscosity (η_0) being reached with the microemulsions showing the highest biopolymer concentration (3%). For higher shear rates, disruption predominates over the formation of new entanglements, molecules align in the direction of flow, and the apparent viscosity decreases with increasing shear rate. As a result, the shear rate ($\dot{\gamma}_c$) corresponding to the transition from Newtonian to shear-thinning behavior presents a slow tendency towards lower values as the biopolymer concentration increases (Fig. 2).

The parameter c is related to the slope of the power law region; thus, it yields information on the shear thinning character of the system. The values of c have also been summarized in Table II. In the case of the microemulsions with xanthan, the mean power law index (n) is about 0.16, and quite similar to the n value obtained for other gums.[28] As it has been commented above, intermolecular association among polymer chains are probably the cause of the formation of a complex network. These weak bound aggregates are progressively disrupted under the influence of shear, thus the pronounced

TABLE II
Parameters of the Carreau Model for the Microemulsions with Xanthan and Chitosan ($r > 0.998$)

Conc. (%, w/w)	Xanthan			Chitosan		
	Viscosity (η_0, Pa s)	$\dot{\gamma}_c \times 10^3$ (s^{-1})	c ($\pm$0.01)	Viscosity (η_0, Pa s)	$\dot{\gamma}_c \times 10^3$ (s^{-1})	c ($\pm$0.001)
0.5	618 ± 8	1.73 ± 0.08	0.40	0.55 ± 0.03	81 ± 7	0.065
1	4050 ± 40	1.53 ± 0.13	0.43	1.17 ± 0.02	39 ± 3	0.069
1.5	7430 ± 60	1.30 ± 0.04	0.42	3. 02 ± 0.09	18± 2	0.063
2	17900 ± 200	1.00 ± 0.04	0.42	11.88 ± 0.08	16 ± 4	0.090
2.5	29000 ± 400	1.11± 0.09	0.43	33.30 ± 0.15	14 ± 9	0.132
3	50700 ± 600	1.13 ± 0.07	0.45	48.03 ± 0.14	19 ± 5	0.138

Results are the mean ± standard deviations ($n = 3$).

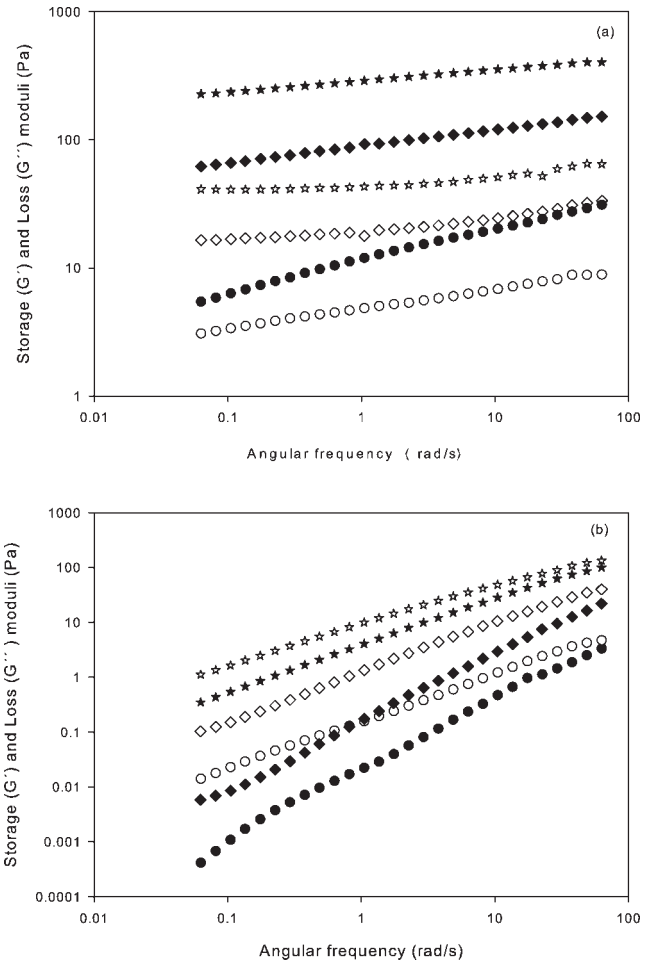

Figure 3 G' (filled symbols) and G'' (open symbols) as a function for all microemulsions with xanthan (a) and chitosan (b) at different concentrations: 0.5% (●,○), 1.5% (◆,◇) and 3% (★,☆).

pseudoplasticity of xanthan solutions.[27] On the other hand, in the case of microemulsions with chitosan at lower concentration, the n value is close to 1 ($n \approx 0.8$), so the behavior of this vehicle could be considered overall as quasi-Newtonian.

Oscillatory test

The experimental values of the mechanical spectra for three different concentrations of biopolymer in the microemulsions studied, obtained in the region of linear behavior, are shown in Figure 3. In the microemulsions with xanthan [Fig. 3(a)], the behavior was predominantly more elastic because G' was greater than G'' in the entire angular frequency ($\omega = 2\pi\nu$) interval studied. Therefore, the loss tangent ($\tan \delta = G''/G'$) was less than 1, and these values decrease with increasing xanthan concentration. This is an indication that a gel-like structure is present.[29] This result is in agreement with published reports where a gel-like structure was also found at xanthan concentrations of 0.5 and 1%.[19] The prevalence of an elastic over a viscous nature in gelled systems could be considered an advantage for the development of bioadhesive systems.[30] However, in the microemulsions with chitosan [Fig. 3(b)], the values of G'' are greater than those of G', for all concentrations studied. Therefore, the loss tangent was greater than 1. This is indicative of a liquid-like solution, and the moduli at the same frequency increase with increasing concentration. These phenomena can be explained by macromolecular entanglement. Since higher concentrations increase entanglement density (the number of intermolecular contacts per unit volume), the viscoelastic properties increase correspondingly.

On the other hand, from the values of G' and G'' we obtained the complex viscosity (η^*) for all the vehicles studied. Figure 4(a,b) shows the plots $\eta^* = f(\omega)$ for the all microemulsions. The η^* values decrease as the angular frequency increases. In contrast, the η^* values increase as the polymer concentration increase.

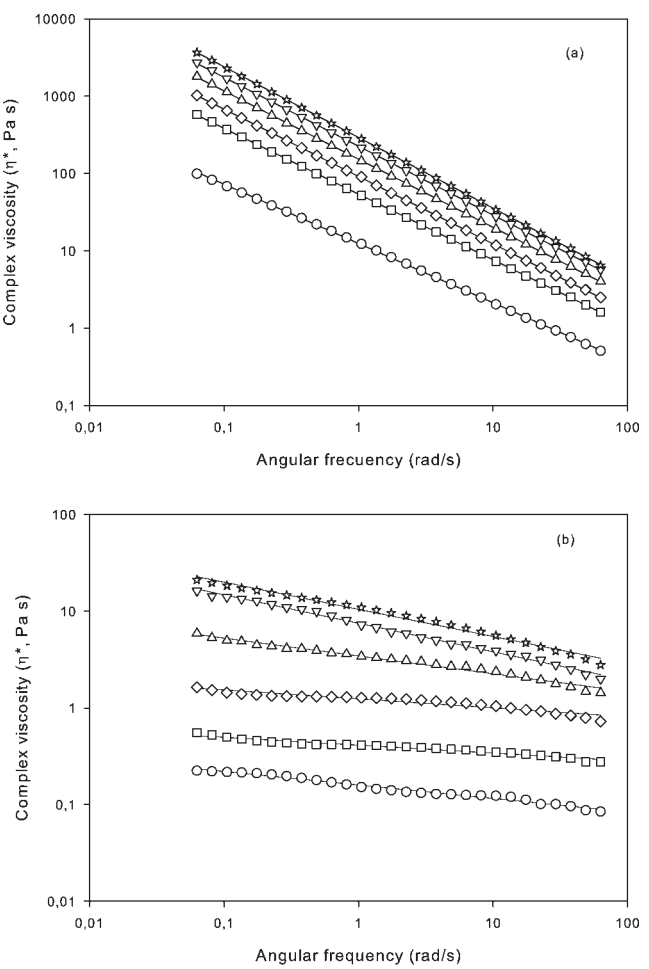

Figure 4 Complex viscosity as a function of angular frequency for microemulsions with xanthan (a) or chitosan (b) at different concentrations: 0.5% (-o-), 1% (-□-), 1.5% (-◇-), 2% (-Δ-), 2.5% (-▽-) and 3% (-☆-).

TABLE III
Power fits for G' and $\eta*$ as function of ω ($r > 0.999$) and Values of Parameters C and α for the Generalized Cox-Merz rule for Microemulsions with Xanthan

Xanthan concentration (%, w/w)	$G' = K' \cdot \omega^{n'}$		$\eta^* = K \cdot \omega^{n-1}$		$\eta^*(\omega) = C\left\{\left[\eta \cdot \left(\dot{\gamma}\right)\right]^{\alpha}\right\}_{\omega=\dot{\gamma}}$	
	K' (Pa)	n'	K (Pa/s^n)	n	C	α
0.5	11.4 ± 0.2	0.247 ±0.008	12.8 ± 0.5	0.232 ± 0.005	2.71 ± 0.04	0.959 ± 0.002
1	51.9 ±0.5	0.154 ± 0.006	57.6 ± 0.9	0.151 ± 0.008	2.70 ± 0.01	0.985 ± 0.006
1.5	89.1 ± 0.1	0.129 ± 0.004	87.4 ± 1.1	0.129 ± 0.006	2.51 ± 0.05	1.054 ± 0.005
2	166 ± 1	0.111 ± 0.004	161 ± 3	0.114 ± 0.003	2.42 ± 0.02	1.067 ± 0.002
2.5	227 ± 3	0.111 ± 0.002	229 ± 5	0.110 ± 0.001	2.07 ± 0.01	1.033 ± 0.003
3	288 ± 5	0.086 ± 0.001	281 ± 4	0.088 ± 0.001	1.92 ± 0.03	1.030 ± 0.001

For all the systems, the values of $\eta^* = f(\omega)$ have been perfectly fitted by power functions of the following kind:

$$\eta^* = K \cdot \omega^{n-1} \tag{8}$$

where K and n are parameters determined experimentally. All the tracings are practically line parallel, thus indicating that the η^* values of all the systems are similarly sensitive to changes in the oscillation frequency [Fig. 4(a,b).

In addition, the storage modulus (G') and loss modulus (G'') have also been perfectly fitted by the following power functions:

$$G' = K' \cdot \omega^{n'} \tag{9}$$

$$G'' = K'' \cdot \omega^{n''} \tag{10}$$

where K', K'', n', and n'' are also parameters determined experimentally. The dependence of G' and G'' on frequency (ω) shows a good fit to the experimental data ($r > 0.996$). The results have been summarized in Table III (microemulsions with xanthan) and Table IV (microemulsions with chitosan).

In the case of microemulsions with xanthan, the exponent of G' in the power law, n', shows no significant differences with the value of n for η^* (Table III). This finding coincides with the observations of other authors,[31] and is logical because on considering that $G'' \ll G'$, it can be affirmed that $\eta^* \cong G'/\omega$ for weak gels. Also, in the microemulsions with chitosan, the exponent of G'' in the power law, n'', also coincided with the value of n for η^* (Table IV), though in this case $G'' \gg G'$. This therefore confirms that it is characteristic of solutions ($\eta^* \cong G''/\omega$).

Correlation of dynamic and steady shear properties

The importance of the Cox-Merz rule is that it relates linear and nonlinear viscoelastic properties. Therefore, shear viscosity information can be derived when only linear viscoelastic data are available, and *vice versa*. The apparent viscosity values in the steady shear (η) and the complex viscosity values (η^*) in oscillatory shear for the microemulsions with xanthan and chitosan, at equal values of shear rate and frequency, were correlated using the generalized Cox-Merz rule,[32] in the following form [eq. (10)]:

$$\eta^*(\omega) = C\{[\eta \cdot (\dot{\gamma})]^{\alpha}\}_{\omega=\dot{\gamma}} \tag{11}$$

where C and α are parameters to be determined on an experimental basis for each system. The values of the parameters of that relation [eq. (10)] for microemulsions with xanthan are given in Table III. The coefficient correlation values are >0.999, and this indicates that the fits are excellent. Therefore,

TABLE IV
Power Fits for G'' and $\eta*$ as Function of ω ($r > 0.999$) and Values of Parameters C and α for the Generalized Cox-Merz Rule for Microemulsions with Chitosan

Chitosan concentration (%, w/w)	$G'' = K''. \omega^{n''}$		$\eta^* = K \cdot \omega^{n-1}$		$\eta^*(\omega) = C\left\{\left[\eta \cdot \left(\dot{\gamma}\right)\right]^{\alpha}\right\}_{\omega=\dot{\gamma}}$	
	K' (Pa)	n'	K (Pa/s^n)	n	C	α
0.5	0.16 ± 0.01	0.855 ± 0.003	0.16 ± 0.02	0.860 ± 0.005	0.37 ± 0.02	0.62 ± 0.021
1	0.41 ± 0.03	0.904 ±0.006	0.41 ± 0.04	0.900 ± 0.002	0.52 ± 0.03	0.64 ± 0.012
1.5	1.21 ± 0.03	0.893 ± 0.005	1.24 ± 0.05	0.907 ± 0.004	0.85 ± 0.07	0.74 ± 0.011
2	6.86 ± 0.05	0.668 ± 0.002	6.94 ± 0.07	0.684 ± 0.001	0.56 ± 0.02	1.02 ± 0.03
2.5	7.61 ± 0.08	0.694 ± 0.001	7.77 ± 0.06	0.721 ± 0.002	0.41 ± 0.01	1.06 ± 0.04
3	8.85 ± 0.02	0.706 ± 0.002	9.70 ± 0.08	0.731 ± 0.001	0.56 ± 0.02	0.98 ± 0.05

microemulsions with xanthan follow the generalized Cox-Merz rule and show greater divergences at high shear with $|\eta^*| > \eta$. As indicated by Soltero et al.,[33] η^* is usually larger than η, since structure is usually disturbed to a lesser extent by the small-amplitude dynamic tests than by steady shear tests. In fact, the C parameter values are >1, and these values decrease as the xanthan concentration increases. On the other hand, the α values are practically equal to 1, which indicates that in the studied cases the generalized Cox-Merz rule can be reduced to a one-parameter linear function $|\eta^*|(\omega) = C.\eta(\dot{\gamma})|_{\omega=\dot{\gamma}}$, called the extended or modified Cox-Merz rule.[34] Thus, a relationship between the C parameter values and xanthan concentrations (c) has been obtained: $C = (2.76 \pm 0.04) - (0.097 \pm 0.008)\ c^2$ ($r > 0.987$). Therefore, the modified Cox-Merz rule can be expressed as follows:

$$\eta^* = [(2.76 \pm 0.04) - (0.097 \pm 0.008) \cdot c^2] \cdot \eta \qquad (12)$$

Taking into account the xanthan concentrations (c), it is possible to determine, from eq. (11), the η^* values once the ηvalues are known, when the measurements are made with a common viscometer or η^* values from the oscillatory measurements that allow the determination of η_a values. While the Cox-Merz rule is applicable to several synthetic and biopolymer dispersions, it is unsuitable for biopolymer dispersions with hyperentanglements (i.e., high density entanglements) or aggregates.[35] In this case, the data deviated from the Cox-Merz rule could be interpreted in terms of specific interpolymer chain interactions, occurring in addition to entanglements and reflecting gel-like behavior.[36]

On the other hand, the values of parameters C and α for microemulsions with chitosan are given in Table IV. The correlation coefficient (r) values are greater than 0.996 for the highest chitosan concentrations (from 2 to 3%). However, the lowest chitosan concentrations have provided correlation coefficient values that are not very satisfactory ($r > 0.95$), due to the slight consistency of the less concentrated systems. For this reason, $\eta^* = f(\eta)$, obtained for all concentrations, has been fitted again to the generalized Cox-Merz rule [eq. (10)]. The following expression has been obtained:

$$\eta^* = (0.64 \pm 0.02) \cdot \eta^{(0.998 \pm 0.01)} \qquad (13)$$

In this case, the correlation coefficient ($r > 0.998$) is better than in the first individual results. Taking into account that the α value is practically equal to 1 [eq. (12)], the generalized Cox-Merz rule can also be reduced to a one-parameter linear function as in the previous case. Therefore, microemulsions with chitosan could be said to also follow the extended Cox-Merz rule. However, in this case the η values were higher than those of η^* (the C parameter < 1), indicating that the Cox-Merz rule is likewise not

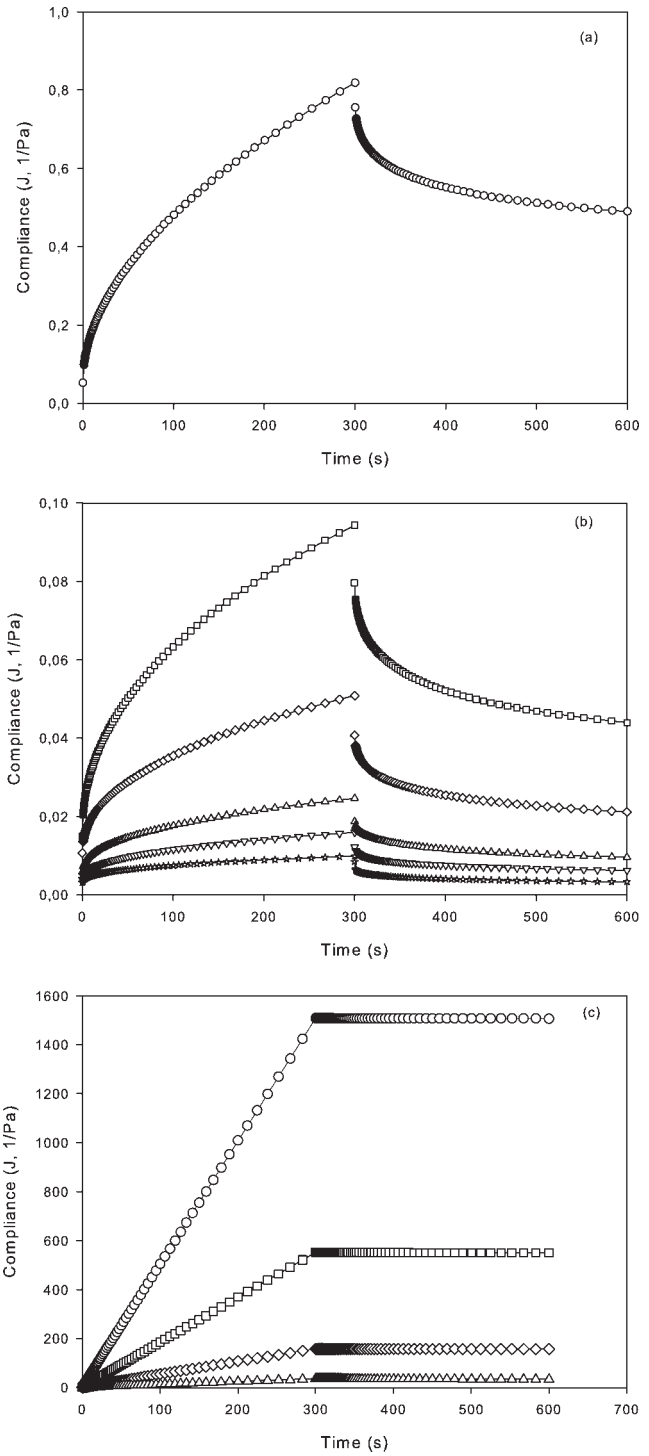

Figure 5 Creep and recovery compliance curves of microemulsions for different concentrations of polymer. With xanthan: (a) 0.5% (-o-) and (b) 1% (-□-), 1.5% (-◇-), 2% (-Δ-), 2.5% (-▽-) and 3% (-☆-) and with chitosan: c) 0.5% (-o-), 1% (-□-), 1.5% (-◇-) and 2% (-Δ-).

TABLE V
Elastic Moduli (G_0, G_1) and Dashpot Viscosities (η_0 and η_1), using the Mechanical Burger's Model for Microemulsion with Xanthan ($r > 0.997$) and the Mechanical Maxwell's Model for Microemulsion with Chitosan ($r > 0.997$)

Conc. (%, w/w)	Xanthan			Chitosan		
	G_0 (Pa)	G_1 (Pa)	η_0 (Pa s)	η_1 (Pa s)	G_0 (Pa)	η_0 (Pa s)
0.5	10.2 ± 0.2	4.7 ± 0.1	571 ± 10	141 ± 1	0.64 ± 0.03	0.1990 ± 0.0001
1.0	47.8 ± 0.6	38.7 ± 1.0	5980 ± 130	1022 ± 2	1.10 ± 0.09	0.5440 ± 0.0001
1.5	72.8 ± 0.8	75.0 ± 1.9	11900 ± 300	1864 ± 3	1.35 ± 0.09	1.892 ± 0.002
2.0	138.2 ± 1.3	156 ± 4	25600 ± 600	3563 ± 5	1.73 ± 0.13	8.43 ± 0.04
2.5	202.8 ± 1.9	242 ± 6	41200 ± 900	5435 ± 7	1.99± 0.15	22.84 ± 0.22
3.0	268.3 ± 2.1	412 ± 10	76600 ± 2100	9464 ± 14	3.33± 0.25	24.48 ± 0.15

applicable to microemulsions with chitosan. Similar departures from the Cox-Merz rule (i.e., $|\eta^*| < \eta$) were also found in other polysaccharide studies.[37–39]

Creep and recovery

Creep and recovery analysis has been carried out for all these systems, to understand the internal structure of the microemulsion formulations. The time dependence of compliance, J, of the microemulsion with xanthan is shown in Figure 5(a,b). For the lowest xanthan concentration (0.5%, w/w) (Fig. 5(a)), the network is weaker than in the case of the rest of the microemulsions [Fig. 5(b)], giving rise to compliance values lower than the value obtained for the smallest polymer concentration. These differences have made it necessary to use another graph. The elasticity of the system increases as the xanthan concentration increases, with a small initial and instantaneous deformation for the highest concentrations of xanthan (3%). This graph suggests elongation and orientation of the polymer chains, involving the breaking and reforming of secondary bonds (i.e., hydrogen bonds). Also, the time dependence of compliance, J, for the microemulsions with chitosan is shown in Figure 5(c). This graph is characteristic of liquid-like solutions, producing a linear response in the creep analysis, and a practical absence of recovery when the stress is removed.

All the creep curves for microemulsions with xanthan were fitted to Burger's model [eq. (3)]. The values of the elastic moduli, G_0 and G_1, and the dashpot viscosities, η_0 and η_1, are shown in Table V. The elastic moduli increase with the xanthan concentration, and the residual viscosity (η_0) is significantly affected by the biopolymer concentration and the same order to the zero-shear viscosity (Table II). This behavior could be interpreted in terms of specific polymeric chain interactions, reflecting gel-like behavior.[31] However, in view of the results obtained for microemulsions with chitosan, the creep curves should be fitted to simple patterns such as Maxwell's model [eq. (4)]. The values of the elastic moduli, G_0, and the dashpot viscosities, η_0, are also shown in Table V. In the same way, the residual viscosity (η_0) is significantly affected by biopolymer concentration, and is quite similar to zero-shear viscosity (Table II). Thus, the G_0 results (Table V) demonstrate that the microemulsions with chitosan show less elastic behavior than the microemulsions with xanthan. All results are consistent with those previously obtained from oscillatory measurements.

The compliance values and total percentage recovery (R, %) for microemulsions with xanthan are shown in Table VI. For the system formulated with the lowest concentration (0.5%), the contribution of the spring of Maxwell is negligible (showing a percentage deformation J_0/J_{MAX} of only 0.07%) and the dashpot of Maxwell corresponds the largest percentage of deformation ($J_\infty/J_{MAX} = 53.6\%$). Therefore, it will be deformed and will flow easily when constant stress is applied to this system. The system only

TABLE VI
J_{MAX}, J_∞, J_{KV}, and J_0 Compliance Values and Total Recovery Percentage [$R = ((J_{Max} - J_\infty)/J_{Max}) \times 100$] for Microemulsions with Xanthan

Xanthan Conc. (%)	$J_{MAX} \times 10^3$ (Pa^{-1})	$J_\infty \times 10^3$ (Pa^{-1})	$J_{KV} \times 10^3$ (Pa^{-1})	$J_0 \times 10^3$ (Pa^{-1})	R (%)
0.5	819 ± 10	439.2 ± 2.5	323 ± 3	57 ± 4	46.4 ± 0.3
1.0	94.4 ± 2.2	35.67 ± 0.37	45.7 ± 0.4	13.0 ± 1.3	62.2 ± 0.5
1.5	50.8 ± 1.2	17.18 ± 0.24	24.0 ± 0.3	9.6 ± 0.6	66.1 ± 0.3
2.0	24.6 ± 0.3	7.73 ± 0.08	11.15 ± 0.11	5.74 ± 0.11	68.6 ± 0.6
2.5	15.9 ± 0.2	4.73 ± 0.07	7.55 ± 0.08	3.64 ± 0.05	70.3 ± 1.5
3.0	9.83 ± 0.09	1.03 ± 0.03	7.47 ± 0.05	1.33 ± 0.02	89.5 ± 1.5

Results are the mean ± standard deviations in brackets ($n = 3$).

recovers 46.4% of its initial form, since the deformation taking place in the dashpot of Maxwell is irreversible. The total percentage recovery (R, %) increases as the concentration of xanthan increases (Table VI), reaching practically 90% for the systems with the highest xanthan concentration (3%, w/w).

Release of progesterone

The drug delivery rate potential of microemulsions with given constituents has been demonstrated to be dependent on the internal mobility of the drug within the vehicle, which is determined by the composition and internal structure of the microemulsion.[40] In this study, the release of progesterone from microemulsions has been examined. Because of the presence of progesterone, a lipophilic drug, within the oil droplets, i.e., the internal phase of the microemulsions, release could be the result of two sequential steps. A first step is the partition from oil internal phase of progesterone to aqueous external phase, while the second step corresponds to diffusion through the aqueous external phase. In our case, the external aqueous phase is added with a biopolymer, xanthan and chitosan, respectively. The presence of the biopolymer could modify the viscosity and also the structure of this aqueous phase, and consequently it could be reflected in diffusion of the drug.

The release of progesterone from microemulsions with two different concentrations of biopolymers (1 and 2%) is shown in Figure 6. The fitting of the release profiles according to the Power law equation ($y = Kt^n$) is reported in Table VII. The fit was quite good considering the correlation coefficient values (r) – all of which approached 1. The exponents, n, related to drug release kinetics, in all cases range from 0.84 to 0.95. These differences in n values could be attributed to the different structure of the aqueous phase for the two types of biopolymers used. In fact, xanthan microemulsions behave as weak gels, while chitosan microemulsions are liquid-like solutions. In addition, these values differ from the ideal value of 0.5, indicating diffusion-controlled drug release (Fickian diffusion mechanism), and are close to 1, which is indicative of drug release independent of time (zero order release kinetics). Consequently, it seems that there is an overlap of both mechanisms.

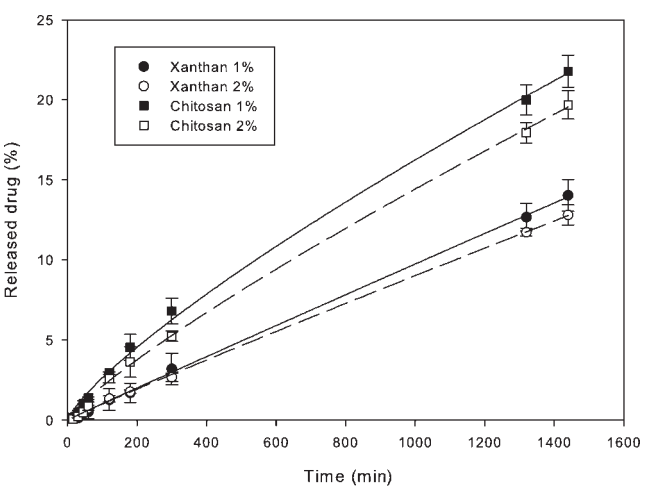

Figure 6 Release profiles of progesterone from microemulsión with xanthan gum (1 and 2%, w/w) and chitosan (1 and 2%, w/w).

TABLE VII
Results of the Regression for the Drug Release Data Generated by the Power Law Equation

	$K \times 10^4$	n	r
Xanthan 1%	1.4 ± 0.2	0.95 ± 0.03	0.9995
Xanthan 2%	1.3 ± 0.1	0.94 ± 0.06	0.9996
Chitosan 1%	5.5 ± 0.4	0.84 ± 0.02	0.9996
Chitosan 2%	3.3 ± 0.3	0.88 ± 0.05	0.9997

(Mean and standard deviation were calculated from three replicates)

On the other hand, as has been commented previously, K is a constant reflecting structural and geometric characteristic of the device. In our study, the K values do not show significant differences in relation to biopolymer concentration (1 and 2%) for the xanthan microemulsions, in the analyzed time interval. However, there are significant differences ($P > 0.5$) for chitosan microemulsions. In addition, the K values are greater for chitosan microemulsions than for xanthan microemulsions (Table VII). These results are in harmony with the differences in their respective η_0 values (Table II).

CONCLUSIONS

For all preparations, shear-thinning behavior was observed and zero shear viscosity (η_0) increased with the biopolymer concentration. The results from the dynamic experiments showed the behavior of microemulsions with chitosan to be characteristic of liquid-like solutions, while the microemulsions with xanthan gum can be regarded as weak gels. The Creep analysis confirms that the microemulsions with chitosan show less elastic behavior than the microemulsions with xanthan gum. Therefore, the prevalence of elastic over viscous nature in gelled systems could be considered an advantage for the development of bioadhesive systems. On the other hand, the progesterone release rate is greater for chitosan microemulsions than for the xanthan gum. In both cases, the release of progesterone is independent of the time and the different K values of the drug are a consequence of the differences in the viscosity and also the structure of the aqueous phase in

the corresponding microemulsions. Therefore, these formulations might be candidates for further research to confirm their usefulness in comparison with the cream formulations.

References

1. Schmidt, J. B.; Blinder, M.; Macheiner, W.; Kainz, C.; Gitsch, G.; Bieglmayer, C. Maturitas 1994, 20, 25.
2. Varila, E.; Rantala, I.; Oikarinen, A.; Risteli, J.; Reunala, T.; Oksanen, H.; Punnonen, R. Br J Obstet Gyneacol 1995, 102, 985.
3. Schmidt, J. B.; Binder, M.; Demeschik, G.; Bieglmayer, C.; Reiner, A. Int J Dermatol 1996, 35, 669.
4. Holzer, G.; Riegler, E.; Honigsmann, H.; Farokhnia, S.; Schmidt, B. Br J Dermatol 2005, 153, 626.
5. Pranked, R. J.; Stella, V. J. Parenter Sci Technol 1990, 44, 139.
6. Kreilgaard, M. Adv Drug Deliv Rev 2002, 54 (Suppl. 1), S77.
7. Trotta, M.; Pattarino, F.; Ignoni, T. Eur J Pharm Biopharm 2002, 53, 203.
8. Valenta, C.; Schultz, K. J Control Release 2004, 95, 257.
9. Trotta, M.; Pattarino, F.; Gasco, M. R. Pharm Acta Helv 1996, 71, 135.
10. Kriwet, K.; Müller-Goymann, C. C. Int J Pharm 1995, 125, 231.
11. Dreher, F.; Walde, P.; Walther, P.; Wehrli, E. J. J Control Release 1997, 45, 131.
12. Williams, A. C.; Barry, B. W. Adv Drug Deliv Rev 2004, 56, 6003.
13. Felt, O.; Furrer, P.; Mayer, J. M.; Plazonnet, B.; Buri, P.; Gurny, R. Int J Pharm 1999, 180, 185.
14. He, P.; Davis, S. S.; Illum, L. Int J Pharm 2004, 166, 75.
15. Ueno, H.; Mori, T.; Fujinaga, T. Adv Drug Deliv Rev 2001, 52, 105.
16. Liu, X. F.; Guan, Y. L.; Yang, D. Z.; Li, Z.; Yao, K. D. J Appl Polym Sci 2001, 79, 1324.
17. Kang, K. S.; Pettit, D. J.In Industrial Gums. Polysaccharides and Their Derivates; Whistler, R. L., Bemiller, J. N., Eds.; Academic Press, New York, 1993; Chapter 13, p 341.
18. Li, J.; Xu, Z. J Pharm Sci 2002, 91, 1669.
19. Talukdar, M. M.; Vinckier, I.; Moldenares, P.; Kinget, R. J Pharm Sci 1996, 85, 537.
20. Dolz, M.; Hernandez, M. J.; Casanovas, A.; Delegido, J. J Appl Polym Sci 2004, 102, 2653.
21. Sittikijyothin, W.; Torres, D.; Gonçalves, M. P. Carbohydr Polym 2005, 59, 339.
22. Diez-Sales, O.; Dolz, M.; Hernàndez, M. J.; Casanovas, A.; Herraez, M. J Appl Polym Sci 2007, 105, 2121.
23. Dolz, M.; Hernandez, M. J.; Delegido, J.; Alfaro, M. C.; Muñoz, J. J Food Eng 2007, 81, 179.
24. Diez-Sales, O.; Garrigues, T. M.; Herraez, J. V.; Belda, R.; Martìn-Villodre, A. J Pharm Sci 2004, 94, 1039.
25. Siepmann, J.; Peppas, N. A. Adv Drug Deliv Res 2001, 58, 139.
26. Lidholm, J.; Johansson, M.; Fornstedt, T. J Chromatogr B 2003, 791, 323.
27. Kang, K. S.; Pettit, D. J.In Industrial Gums. Polysaccharides and Their Derivatives, 3th ed.; Whistler, R. L., BeMiller, J. N., Eds.; Academic Press: San Diego, CA, 1993; p 341.
28. Dolz, M.; Hernández, M. J.; Delegido, J. J Appl Polym Sci 2006, 102, 897.
29. Xu, X.; Liu, W.; Zang, L. Food Hydrocolloids 2006, 20, 723.
30. Oechsner, M.; Keipert, S. Eur J Pharm Biopharm 1999, 47, 113.
31. Cabeza, C.; Muñoz, J.; Alfaro, M. C.; Flores, V. In Progress in Rheology: Theory and Applications; Martínez Boza, F. J., Guerrero, A., Partal, P., Franco, J. M., Muñoz, J. H., Eds; grupo Español de Reología: Seville 2002; p 477.
32. Juszczak, L.; Witczak, M.; Fortuna, T.; Banys, A. J. J Food Eng 2004, 63, 209.
33. Soltero, J. F. A.; Robles-Vazquez, O.; Puig, J. E. J Rheol 1995, 39, 235.
34. Gunasekaran, S., Ak, M. M. Trends Food Sci Technol 2000, 11, 115.
35. Chamberlain, E. K.; Rao, M. A. Carbohydr Polym 1999, 40, 25129.
36. Rochefort, W. E.; Middleman, S. J Rheol 1987, 31, 337.
37. Da Silva, P. M. S.; Oliveira, J. C.; Rao, M. A. Int J Food Properties 1998, 1, 23.
38. Zimeri, J. E.; Kokini, J. L. Carbohydr Polym 2003, 52, 67.
39. Yu, H.; Huang, Y.; Ying, H.; Xiao, Ch. Carbohydr Polym 2007, 69, 29.
40. Kogan, A.; Garti, N. Adv in Colloid Interface Sci 2006, 123–126, 369.